Pseudo-proper ferroelectricity and magnetoelectric effects in $TbMnO_3$

Pierre Tolédano*
Laboratory of Physics of Complex Systems, University of Picardie, 33 rue Saint-Leu, 80000 Amiens, France
(Received 14 January 2009; published 17 March 2009)

A unifying theoretical description of the magnetoelectric effects found in $TbMnO_3$ is proposed. The phase diagrams at zero and applied magnetic fields are worked out. They reveal that the "giant" dielectric effects observed in the spiral phase of $TbMnO_3$ result from an effective bilinear coupling of the polarization with the magnetic order parameter. This property applies to a number of multiferroic materials, in which the electric polarization is induced by a spiral magnetic structure. The spiral phase is shown to become unstable above definite threshold fields, giving rise to the observed polarization flops and triggering the onset of a commensurate ferroelectric phase.

DOI: 10.1103/PhysRevB.79.094416 PACS number(s): 77.80.Fm, 75.80.+q, 77.22.Ej, 77.84.Dy

It was recently observed[1] that a spontaneous electric polarization can emerge at a magnetic transition if the magnetic spins order in noncollinear spiral structures.[2] This new type of magnetostructural transition was reported in various classes of the so-called multiferroic materials,[3,4] in which the correlation between spin and dipole orderings results in remarkable magnetoelectric effects, denoting a strong sensitivity to the applied magnetic field, such as reversals or flops of the polarization or a strong enhancement of the dielectric constant. On the theoretical ground a number of arguments have been raised[5–7] to justify the observation of magnetoelectric effects in spiral magnets and group theoretical approaches were proposed.[8,9] Here, we give a unifying theoretical description of the magnetoelectric effects found in the manganite $TbMnO_3$, which has been used as a prototype material in most of the theoretical approaches to multiferroics. Using a Landau-type description the phase diagrams at zero and applied magnetic fields are worked out. They show that the dielectric effects observed in the spiral phase of $TbMnO_3$ (Ref. 1) result from an effective *bilinear* coupling of the polarization with the magnetic order parameter. It gives rise to a critical behavior typical of *proper* ferroelectric transitions, with a divergence of the dielectric permittivity and a critical exponent of $\frac{1}{2}$ for the electric polarization, whereas the magnitude of the polarization in the spiral phase is of the order found in *improper* ferroelectrics. This hybrid *pseudo-proper* ferroelectric behavior is characterized by a great sensitivity to an applied magnetic field. In $TbMnO_3$ the observed polarization flops are shown to result from a switching of the spiral phase to a more stable ferroelectric phase, which triggers the onset of a commensurate structure. The explicit critical behavior of the pertinent physical quantities is worked out.

Let us first describe the phase diagram of $TbMnO_3$ in the absence of applied magnetic field. The $Pbnm1'$ paramagnetic (P) symmetry of $TbMnO_3$, above 41 K, has four bidimensional irreducible corepresentations (ICs) (Ref. 10) associated with the incommensurate wave vector $\vec{k}=(0,k,0)$ with $k\approx 0.28$. Neutron-diffraction results[11] show that two among the four ICs, denoted hereafter Δ_2 and Δ_3, are involved in the symmetry-breaking mechanisms occurring at the 41 and 28 K transitions. The generators of Δ_2 and Δ_3 are given in Table I. The complex amplitudes corresponding to the magnetic waves transforming according to Δ_2 and Δ_3 can be written, respectively, as $\bar{S}_2=S_2e^{i\Theta_2}$, $\bar{S}_2^*=S_2e^{-i\Theta_2}$ and $\bar{S}_3=S_3e^{i\Theta_3}$, $\bar{S}_3^*=S_3e^{-i\Theta_3}$. It yields the following set of basic order-parameter invariants: $\mathfrak{I}_1=S_2^2$, $\mathfrak{I}_2=S_3^2$, and $\mathfrak{I}_3=S_2^2S_3^2\cos 2\varphi$ with $\varphi=\Theta_2-\Theta_3$. The corresponding free-energy density reads

$$\Phi_1(S_2,S_3,\varphi)=\Phi_0(T)+\frac{\alpha_1}{2}\mathfrak{I}_1+\frac{\beta_1}{4}\mathfrak{I}_1^2+\frac{\alpha_2}{2}\mathfrak{I}_2+\frac{\beta_2}{4}\mathfrak{I}_2^2+\frac{\gamma_1}{2}\mathfrak{I}_3+\frac{\gamma_2}{4}\mathfrak{I}_3^2+\cdots, \quad (1)$$

which is an eighth-degree expansion necessary to account for the full set of stable states.[12,13] Minimizing Φ_1 with respect to φ yields the following equation of state:

$$S_2^2S_3^2\sin 2\varphi(\gamma_1+\gamma_2S_2^2S_3^2\cos 2\varphi)=0. \quad (2)$$

Equation (2) and the minimization of Φ_1 with respect to S_2 and S_3 show that *five distinct stable states*, denoted I–V, may arise below the P phase for different equilibrium values of the order parameter. Their symmetries are given in Fig. 1. The theoretical phase diagrams shown in Figs. 2(a)–2(d) indicate the region of stability of each phase. The phases denoted I and II in Figs. 1 and 2 can be identified as the anti-

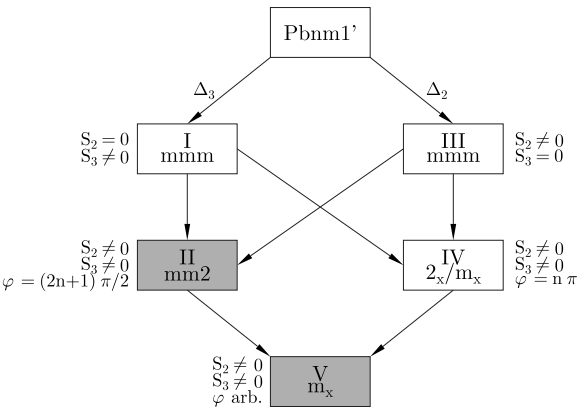

FIG. 1. Crystallographic point groups of phases I–V and corresponding equilibrium conditions fulfilled by the order parameter $(\bar{S}_2,\bar{S}_3)$. Gray rectangles indicate ferroelectric phases.

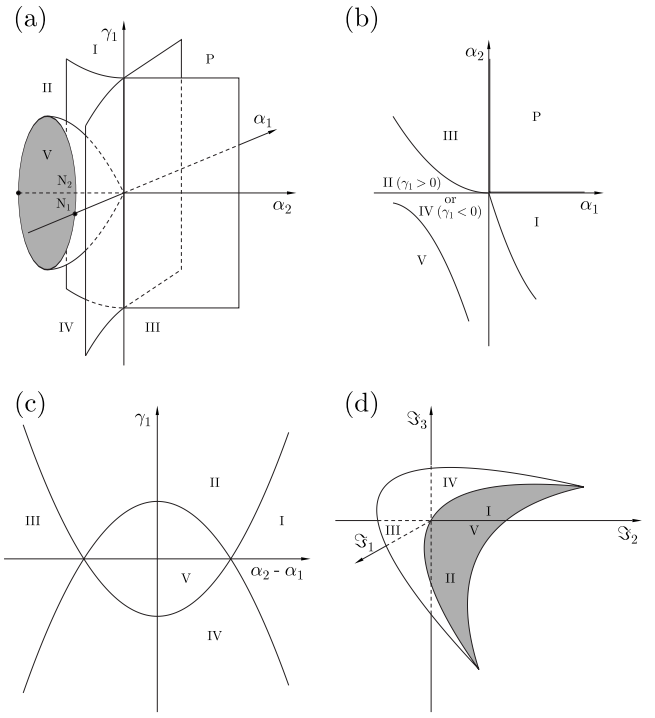

FIG. 2. Phase diagrams at zero field deduced from the minimization of the free energy Φ_1 given by Eq. (1) in (a) the $(\alpha_1,\alpha_2,\gamma_1)$ space, (b) the (α_1,α_2) plane, (c) the $(\gamma_1,\alpha_2-\alpha_1)$ plane, and (d) the orbit space $(\mathfrak{I}_1,\mathfrak{I}_2,\mathfrak{I}_3)$. In (a) the phases are separated by second-order transition surfaces, which become curves in (b) and (c). In (b) and (c) N_1 and N_2 are four-phase points which become lines in (a). In (d) phases I and III and II and IV correspond, respectively, to lines and surfaces, with phase V coinciding with the volume limited by the surfaces. The paramagnetic phase is at the origin of the orbit space.

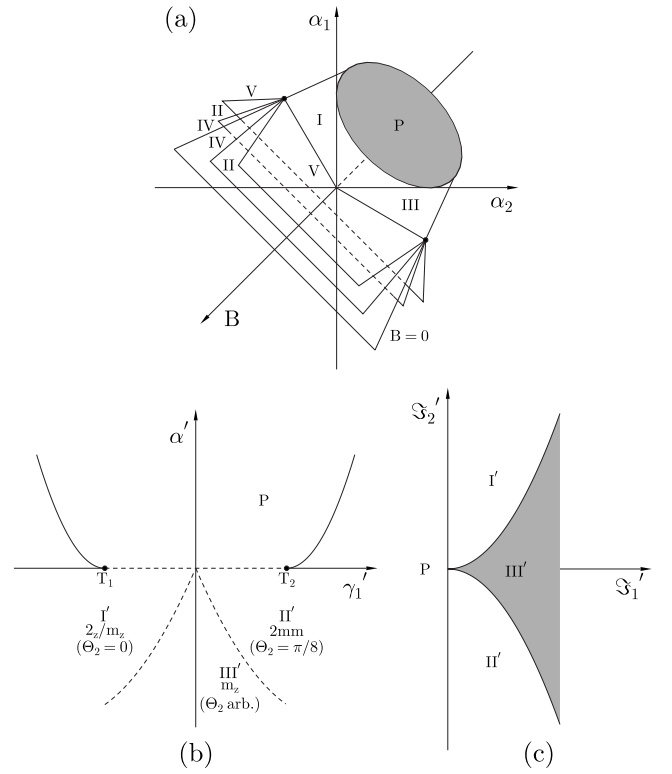

FIG. 3. (a) Phase diagram corresponding to the free energy Φ_1 under applied B_x or B_y field. It shows that above the threshold field B^{th} phase II is shifted to phase V. (b), (c) Phase diagrams associated with the free energy Φ_2, given by Eq. (6) in (b) the (α',γ_1') plane and (c) the orbit space $(\mathfrak{I}_1',\mathfrak{I}_2')$ with $\mathfrak{I}_1'=S_2^2$ and $\mathfrak{I}_2'=S_2^8\cos 8\Theta_2$. In (b) the structural point groups and equilibrium conditions are indicated for phases $I'-III'$. Hatched and solid lines are, respectively, second- and first-order transition lines. T_1 and T_2 are tricritical points.

ferromagnetic phases observed in $TbMnO_3$ below, respectively, $T_1=41$ K and $T_2=28$ K.

Phase I corresponds to $S_3^e=\pm(-\frac{\alpha_2}{\beta_2})^{1/2}$ and $S_2^e=0$. It is induced by Δ_3, in agreement with the neutron-diffraction measurements by Kenzelmann *et al.*,[11] and has the point group *mmm* which allows an antiferromagnetic ordering along y.[1,11] The incommensurate modulation along y is expressed by the invariants $\delta_3 S_3^2\frac{\partial\Theta_3}{\partial y}$ and $\sigma_3[(\frac{\partial S_3}{\partial y})^2+S_3^2(\frac{\partial\Theta_3}{\partial y})^2]$ which yield the equilibrium wave vector $k^e=-\frac{\delta_3}{\sigma_3}$ when assuming $\Theta_3=ky$.

Figure 2 shows that phase II can be reached from phase I across a second-order transition. It corresponds to the equilibrium values $S_2^e=\pm(\frac{\gamma_1\alpha_2+\beta_2\alpha_1}{\gamma_1^2-\beta_1\beta_2})^{1/2}$, $S_3^e=\pm(\frac{\gamma_1\alpha_1+\beta_1\alpha_2}{\gamma_1^2-\beta_1\beta_2})^{1/2}$, and $\varphi=(2n+1)\frac{\pi}{2}$ and to the stability conditions $\gamma_1\geq\gamma_2 S_2^{e2}S_3^{e2}>0$. The polar point group *mm*2 of phase II is consistent with an antiferromagnetic order in the (y,z) planes and a spontaneous polarization component P_z. The dielectric free-energy density $\Phi_1^D=\nu P_z S_2 S_3\sin\varphi+\frac{P_z^2}{2\epsilon_{zz}^0}$ gives the equilibrium polarization

$$P_z^e=\pm\nu\epsilon_{zz}^0 S_2^e S_3^e. \tag{3}$$

Although the symmetry of phase II reflects the coupling of two order parameters $\bar{S}_2$ and $\bar{S}_3$, $\bar{S}_3$ has been already activated at the P→I transition and is *frozen* at the I→II symmetry-breaking mechanism, which is induced by the sole order parameter $\bar{S}_2$. Therefore, Eq. (3) expresses an *effective bilinear coupling* of P_z with $\bar{S}_2$ giving rise to a *proper ferroelectric critical behavior* at the I→II transition characterized by a Curie-Weiss-type divergence of the dielectric permittivity ϵ_{zz} and a critical exponent of $\frac{1}{2}$ for the temperature dependence of P_z. This situation is reminiscent of pseudo-proper ferroelectric transitions[13] where the spontaneous polarization has the same symmetry as the transition order parameter, to which it couples bilinearly, but results from an induced (secondary) mechanism. In the ferroelectric phase of $TbMnO_3$, P_z and $\bar{S}_2$ are related by a *pseudo-proper-like* coupling since they display different symmetries. Putting $\alpha_1=a_1(T-T_0)$ and $\alpha_2=a_2(T-T_1)$, one has for $T\leq T_2$ $S_2^e=\pm\tilde{a}(T_2-T)^{1/2}$ and $S_3^e\cong\pm[\frac{a_2}{\beta_2}(T_1-T_2)]^{1/2}$ with $\tilde{a}=(\frac{a_2\gamma_1+a_1\beta_2}{\gamma_1^2-\beta_1\beta_2})^{1/2}$ and $T_2=\frac{a_1\beta_2 T_0+a_2\gamma_1 T_1}{a_1\beta_2+a_2\gamma_1}$. Therefore, the temperature dependence of P_z^e for $T\leq T_2$ is given by $P_z^e=\pm A(T_2-T)^{1/2}$ with $A=\nu\epsilon_{zz}^0\tilde{a}(\frac{a_2}{\beta_2})^{1/2}(T_1-T_2)^{1/2}$. The dielectric permittivity diverges at T_2, with $\epsilon_{zz}(T)=\epsilon_{zz}^0[1-C\frac{(T_1-T)}{(T-T_2)}]$ for $T>T_2$ and $\epsilon_{zz}(T)=\epsilon_{zz}^0[1-D\frac{(T_1-T_2)}{(T_2-T)}]$ for $T<T_2$ with $C=\frac{\nu^2 a_2\epsilon_{zz}^0}{a_1\beta_2+a_2\gamma_1}$ and $D=C\frac{\gamma_1^2-\beta_1\beta_2}{\gamma_1^2-4\beta_1\beta_2}$. The preceding power laws pro-

TABLE I. Generators of the irreducible corepresentations Δ_2 and Δ_3 of the paramagnetic $Pbnm1'$ space group. $\epsilon=kb/2$ for phases I and II and $\epsilon=\pi/4$ for phase II′. T is the time-reversal symmetry. The corepresentations have been deduced from the irreducible representations of the group $G_k=m2m$, denoted Γ_2 and Γ_3, by Kenzelmann *et al.* (Ref. 11), following the procedure described in Refs. 10 and 13.

$Pbnm1'$		$(U_y \mid \frac{a}{2}\frac{b}{2}0)$	$(\sigma_z \mid 00\frac{c}{2})$	$(I \mid 000)$	T	$(E \mid 0b0)$
Δ_2	$\bar{S}_2$ $\bar{S}_2^*$	$\begin{bmatrix} e^{i\epsilon} & \\ & e^{-i\epsilon} \end{bmatrix}$	$\begin{bmatrix} -1 & \\ & -1 \end{bmatrix}$	$\begin{bmatrix} & 1 \\ 1 & \end{bmatrix}$	$\begin{bmatrix} -1 & \\ & -1 \end{bmatrix}$	$\begin{bmatrix} e^{2i\epsilon} & \\ & e^{-2i\epsilon} \end{bmatrix}$
Δ_3	$\bar{S}_3$ $\bar{S}_3^*$	$\begin{bmatrix} -e^{i\epsilon} & \\ & -e^{-i\epsilon} \end{bmatrix}$	$\begin{bmatrix} 1 & \\ & 1 \end{bmatrix}$	$\begin{bmatrix} & 1 \\ 1 & \end{bmatrix}$	$\begin{bmatrix} -1 & \\ & -1 \end{bmatrix}$	$\begin{bmatrix} e^{2i\epsilon} & \\ & e^{-2i\epsilon} \end{bmatrix}$

vide an excellent fit with the experimental curves reported by Kimura *et al.*[1] A conventional improper trilinear coupling between P_z and the magnetic order parameter would lead to an upward step of ϵ_{yy} at T_2 and a *linear* dependence $P_z \approx (T_2-T)$.[13] Accordingly, the ferroelectric phase of $TbMnO_3$ shows a hybrid behavior, displaying critical anomalies typical of proper ferroelectric transitions, although the magnitude of the induced polarization (≈ 800 μC m^{-2}) is of the order usually found in improper ferroelectrics.[13] Note that Eq. (3) implies switching the sign of P_z with opposite senses for the spiral configuration, as observed by Yamasaki *et al.*[14] Note also that the mixed Lifshitz invariant $P_z(\bar{S}_2\frac{\partial \bar{S}_3^*}{\partial y}-\bar{S}_3\frac{\partial \bar{S}_2^*}{\partial y}) \cong P_z S_2 S_3 k$, assumed by Mostovoy[6] to give rise to P_z, reduces to the effective bilinear coupling expressed by Eq. (3).

Application of a magnetic field along the x or y direction in the spiral phase of $TbMnO_3$ induces drastic changes and remarkable magnetoelectric effects. The spontaneous polarization is switched along the x direction above threshold fields $B_x^{\text{th}}=9$ T and $B_y^{\text{th}} \cong 4.5$ T, respectively,[15] which is a first-order lock-in transition to a commensurate structure occurring with $k=1/4$.[15] Let us show that under B_x or B_y field phase II is switched to a lower symmetry ferroelectric phase, triggering the onset of the lock-in commensurate phase into which the observed polarization flops take place. Taking into account the magnetic free-energy density $\Phi_1^M=\mu_0\frac{M^2}{2}-\vec{M}\vec{B}$, Eq. (2) becomes, under B_x field,

$$S_2^2 S_3^2 \sin 2\varphi(\gamma_1+\gamma_2 S_2^2 S_3^2 \cos 2\varphi-\mu_x B_x^2)=0 \tag{4}$$

with $\mu_x>0$. The stability condition for phase II is $\gamma_1-\gamma_2 S_2^{e2} S_3^{e2} \geq \mu_x B_x^2$, showing that above the threshold field $B_x^{th}=(\frac{\gamma_1-\gamma_2 S_2^{e2} S_3^{e2}}{\mu_x})^{1/2}$, phase II becomes unstable and switches to phase V, as shown in the phase diagram of Fig. 3(a). Under B_x field the magnetic symmetry m_x1' of phase V is lowered to m_x. The magnetoelectric coupling $\kappa_1 P_x M_x M_z S_2 S_3 \sin\varphi$ favors the induced polarization component

$$P_x=-\epsilon_{xx}^0 \kappa_1 \mu_0^{-1} B_x M_z S_2^e S_3^e \sin\varphi_e \tag{5}$$

implying a nonzero magnetic moment M_z and a lowering of the m_x symmetry to triclinic 1, related to a rotation of the spiral above the threshold field. The tendency of the material to stabilize a higher-symmetry structure with a *spontaneous* P_x component triggers the onset of the commensurate $k=1/4$ phase at a first-order lock-in transition. A similar process yields the lock-in structure under B_y field. Above the threshold field $B_y^{th}=(\frac{\gamma_1-\gamma_2 S_2^{e2} S_3^{e2}}{\mu_y})^{1/2}$ phase II shifts to phase V, the symmetry of which is lowered to m_x' under B_y field. The magnetoelectric coupling $\kappa_2 P_x M_x M_y S_2^2 S_3^2 \sin 2\varphi$ lowers the symmetry to triclinic 1 for inducing the polarization component $P_x=-\epsilon_{xx}^0 \kappa_2 \mu_0^{-1} B_y M_x S_2^{e2} S_3^{e2} \sin 2\varphi_e$, which implies a nonzero M_x component, giving rise to the lock-in phase. The existence of an intermediate phase between phase II and the lock-in phase under B_y field is consistent with the observation by Barath *et al.*[16] of a coexistence of distinct structural phases in the intermediate field regime ($B_y=4-7$ T).

The preceding description clarifies the process leading to the formation of a lock-in phase under applied field in $TbMnO_3$ but does not account for the polarization flops observed in this material. Let us assume that the lock-in transition *decouples* the $\bar{S}_2$ and $\bar{S}_3$ order parameters, which are coupled at zero field, and show that a single order-parameter model with $S_2 \neq 0$ and $S_3=0$ explains the vanishing of P_z and correlated onset of P_x which occur in $TbMnO_3$ *within* the commensurate structure. Table I gives the generators of Δ_2 for $k=1/4$. It yields the free-energy density

$$\Phi_2=\frac{\alpha'}{2}S_2^2+\frac{\beta'}{4}S_2^4+\frac{\gamma_1'}{8}S_2^8 \cos 8\Theta_2+\frac{\gamma_2'}{16}S_2^{16}\cos^2 8\Theta_2, \tag{6}$$

which has to be expanded up to 16 degrees.[12,13] The equation of state

$$S_2^8 \sin 8\Theta_2(\gamma_1'+\gamma_2' S_2^8 \cos 8\Theta_2)=0 \tag{7}$$

shows that *three* commensurate phases, denoted I′–III′,

which exhibit a fourfold multiplication of the *b*-lattice parameter, can stabilize at zero field. The corresponding phase diagram [Figs. 3(b) and 3(c)] shows that phase II′, which is stable for $\Theta_2 = \pm \frac{\pi}{8}$ and $\gamma_1' \geq \gamma_2' S_2^{e8} > 0$, has the structural symmetry $2mm$, permitting a spontaneous polarization $P_x^e = \pm \nu' \epsilon_{xx}^0 S_2^{e4}$, deduced from the dielectric free energy $\Phi_2^D = \nu' P_x S_2^4 \sin 4\Theta_2 + \frac{P_x^2}{2\epsilon_{xx}^0}$. The II→II′ lock-in transition is necessarily first order, in agreement with the observations of Aliouane *et al.*[15] Accordingly, the onset of P_x in the lock-in phase occurs after the decrease and vanishing of P_z, not allowed by the symmetry of phase II′, which takes place in the intermediate regime between phase II and the commensurate phase. Note that assuming $S_2 = 0$ and $S_3 \neq 0$ gives an identical result, whereas a coupled order-parameter model $S_2 \neq 0$ and $S_3 \neq 0$ would lead to a lower monoclinic symmetry 2_x for the lock-in phase.

In conclusion, the order-parameter symmetry associated with the magnetostructural transition observed in $TbMnO_3$ clarifies the nature of the induced ferroelectric order observed in this material. It explains the sensitivity of the dielectric behavior under applied magnetic field and the resulting polarization flops. The same hybrid behavior is found in other multiferroic materials such as $DyMnO_3$, $TbMn_2O_5$, $MnWO_4$, or $Ni_3V_2O_8$.[2] In these compounds, as in $TbMnO_3$, the ferroelectric phase does not appear directly below the paramagnetic phase, but below an intermediate nonpolar magnetic phase, i.e., the loss of space inversion does not occur simultaneously with the loss of time-reversal symmetry. The electric polarization results from the coupling of two distinct magnetic order parameters, where one has already been activated in the intermediate phase. As a consequence a pseudo-proper coupling of the polarization with a single symmetry-breaking magnetic order parameter is created, which gives rise to the remarkable dielectric and magnetoelectric properties observed in spiral magnets.

The polarization flops observed in $TbMnO_3$ correspond formally to linear magnetoelectric effects $P_x = \alpha_{11} B_x$ and $P_x = \alpha_{12} B_y$. However, the complex underlying mechanisms of these effects have been shown to occur in two successive steps: a shifting of phase II toward a more stable ferroelectric phase of lower symmetry, above definite threshold fields, followed by a field-induced lock-in to a commensurate phase, where the symmetry of which imposes the vanishing of P_z and the onset of P_x. The observation in $DyMnO_3$ of similar induced flops, not associated with a commensurate high-field phase,[17] implies a stabilization of the induced P_x polarization via magnetoelectric couplings under B_x or B_y fields. The corresponding incommensurate high-field phases acquire the monoclinic 2_x or $2_x'$ magnetic symmetries which yield a vanishing of P_z across the flop transitions.

*pierre.toledano@wanadoo.fr

[1] T. Kimura, T. Goto, H. Shintani, K. Ishizaka, T. Arima, and Y. Tokura, Nature (London) **426**, 55 (2003).
[2] T. Kimura, Annu. Rev. Mater. Res. **37**, 387 (2007).
[3] M. Fiebig, J. Phys. D **38**, R123 (2005).
[4] S.-W. Cheong and M. Mostovoy, Nature Mater. **6**, 13 (2007).
[5] H. Katsura, N. Nagaosa, and A. V. Balatsky, Phys. Rev. Lett. **95**, 057205 (2005).
[6] M. Mostovoy, Phys. Rev. Lett. **96**, 067601 (2006).
[7] I. A. Sergienko and E. Dagotto, Phys. Rev. B **73**, 094434 (2006).
[8] A. B. Harris, Phys. Rev. B **76**, 054447 (2007).
[9] P. G. Radaelli and L. C. Chapon, Phys. Rev. B **76**, 054428 (2007).
[10] O. V. Kovalev, *The Irreducible Representations of Space Groups* (Gordon and Breach, New York, 1965).
[11] M. Kenzelmann, A. B. Harris, S. Jonas, C. Broholm, J. Schefer, S. B. Kim, C. L. Zhang, S. W. Cheong, O. P. Vajk, and J. W. Lynn, Phys. Rev. Lett. **95**, 087206 (2005).
[12] If n is the highest degree of the basic order-parameter invariants the free energy has to be truncated at not less than the degree $2n$ for ensuring the stability of all the phases involved in the phase diagram (Ref. 13). The degree $n=4$ of $\mathfrak{I}_3$ imposes to expand Φ_1 up to the degree $2n=8$. Φ_2 must be expanded at the degree $2n=16$ since $n=8$ for the $\mathfrak{I}_2'$ invariant.
[13] J. C. Tolédano and P. Tolédano, *The Landau Theory of Phase Transitions* (World Scientific, Singapore, 1987).
[14] Y. Yamasaki, H. Sagayama, T. Goto, M. Matsuura, K. Hirota, T. Arima, and Y. Tokura, Phys. Rev. Lett. **98**, 147204 (2007).
[15] N. Aliouane, D. N. Argyriou, J. Strempfer, I. Zegkinoglou, S. Landsgesell, and M. v. Zimmermann, Phys. Rev. B **73**, 020102(R) (2006).
[16] H. Barath, M. Kim, S. L. Cooper, P. Abbamonte, E. Fradkin, I. Mahns, M. Rubhausen, N. Aliouane, and D. N. Argyriou, Phys. Rev. B **78**, 134407 (2008).
[17] J. Strempfer, B. Bohnenbuck, M. Mostovoy, N. Aliouane, D. N. Argyriou, F. Schrettle, J. Hemberger, A. Krimmel, and M. v. Zimmermann, Phys. Rev. B **75**, 212402 (2007).